Building a Ring Resonator Feedback Loop

Parth Patel

Electrical Engineering and Computer Sciences
University of California, Berkeley

July 26, 2022

Acknowledgement

Building a Ring Resonator Feedback Loop

by Parth Patel

Research Project

Submitted to the Department of Electrical Engineering and Computer Sciences, University of California at Berkeley, in partial satisfaction of the requirements for the degree of **Master of Science, Plan II**.

Approval for the Report and Comprehensive Examination:

Committee:

_____

Professor Vladimir Stojanovic
Research Advisor

07/25/2022

_____
(Date)

* * * * * * *

_____

Professor Borivoje Nikolic
Second Reader

7/25/2022
_____
(Date)

Building a Ring Resonator Feedback Loop

By Parth Patel

July 26, 2022

Abstract

Although Magnetic Resonance Imaging(MRI) has changed the world of medicine by providing a non-intrusive method of viewing the human anatomy, its implementation remains bulky and power hungry. The coaxial cables that it uses are oftentimes victims of electromagnetic interference and noise. Furthermore, coaxial cables are unable to transmit data at long distances so most computation must be done locally. Resonant ring resonators(RRM) are an emerging technology that could remove the drawbacks of traditional coaxial cables by providing a low interference and long distance data transmission method. As promising as this sounds, RRMs currently suffer from a low spur free dynamic range(SFDR) which greatly limits their practical usage in various applications, including MRI. One way of tackling this issue is by making the response of the ring resonator more linear through negative feedback. This thesis will cover the basic background of what RRMs are, a description of the circuits and feedback loop used to linearize its response, and experiments carried out to measure improvements in SFDR, bandwidth, etc. Additionally, this project report will serve as a timeline of progress made over the course of the project, from high level simulations to circuit level simulations to finally building out the feedback loop in physical hardware. Ultimately the TIA was fully built and was able to convert photocurrent from the ring drop port to a measurable voltage output.

Contents

1 Introduction

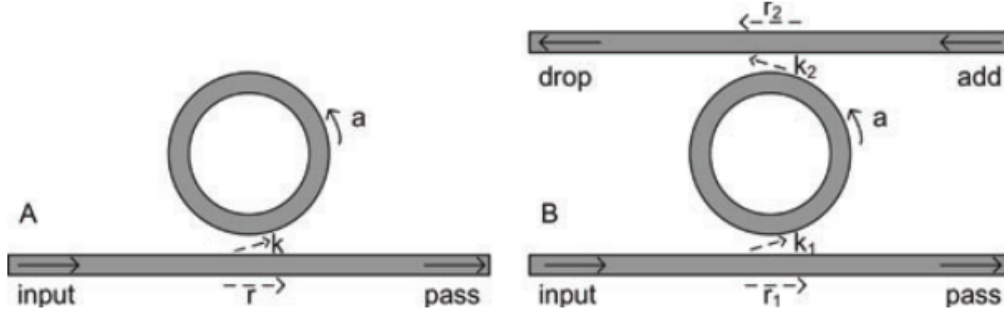## 1.1 Ring Resonator Background

Figure 1: all-pass ring resonator(left), add/drop ring resonator(right)

In its most basic form, a ring resonator is simply a ring-shaped waveguide that allows light to travel into its input port and out of its output port(see Figure 1). The ring itself is essentially a PN junction in the shape of the ring. By modulating the voltage across this PN junction, we can change the resonance frequency of the ring and hence modulate the optical power transmitted out of the output port.

The left hand figure above depicts an all-pass resonator, where r is the self coupling factor, k is the coupling factor. For a lossless coupler we can assume that $r^2 + k^2 = 1$, where r^2 and k^2 can be thought of as the fraction of the total power that travels through the straight waveguide and the ring resonator respectively. The letter "a" coefficient can be thought of as an attenuation factor within the ring(i.e power loss). On the right hand figure, we see that additional drop and add ports can be added to our configuration. This newly formed ring structure is known as an add/drop resonator. The coupling(or self coupling) factors k2 and r2 are exactly analogous to the r and k values discussed for the all-pass resonator. The transmission intensity, in other words the fraction of power that reaches the output relative to the input power, can be expressed as T.

1.

$$T_n = \frac{I_{pass}}{I_{input}} = \frac{r_2^2 a^2 - 2r_1 r_2 a cos(\phi) + r_1^2}{1 - 2r_1 r_2 a cos(\phi) + (r_1 r_2 a)^2}$$

2.

$$T_d = \frac{I_{drop}}{I_{input}} = \frac{(1 - r_1^2)(1 - r_2^2)a}{1 - 2r_1 r_2 a cos(\phi) + (r_1 r_2 a)^2}$$

Note that for the all-pass resonator, critical coupling(i.e resonance conditions) occur when the power entering the ring is equal to the power attenuated within the ring. For an add/drop resonator, the critical coupling conditions occur when the power into the ring is approximately equal to the power transmitted out of the drop port. Now that we know the conditions at which resonance is achieved, we can reason about the transfer characteristics of an actual ring.

1.2 An Example Ring Resonator Sweep
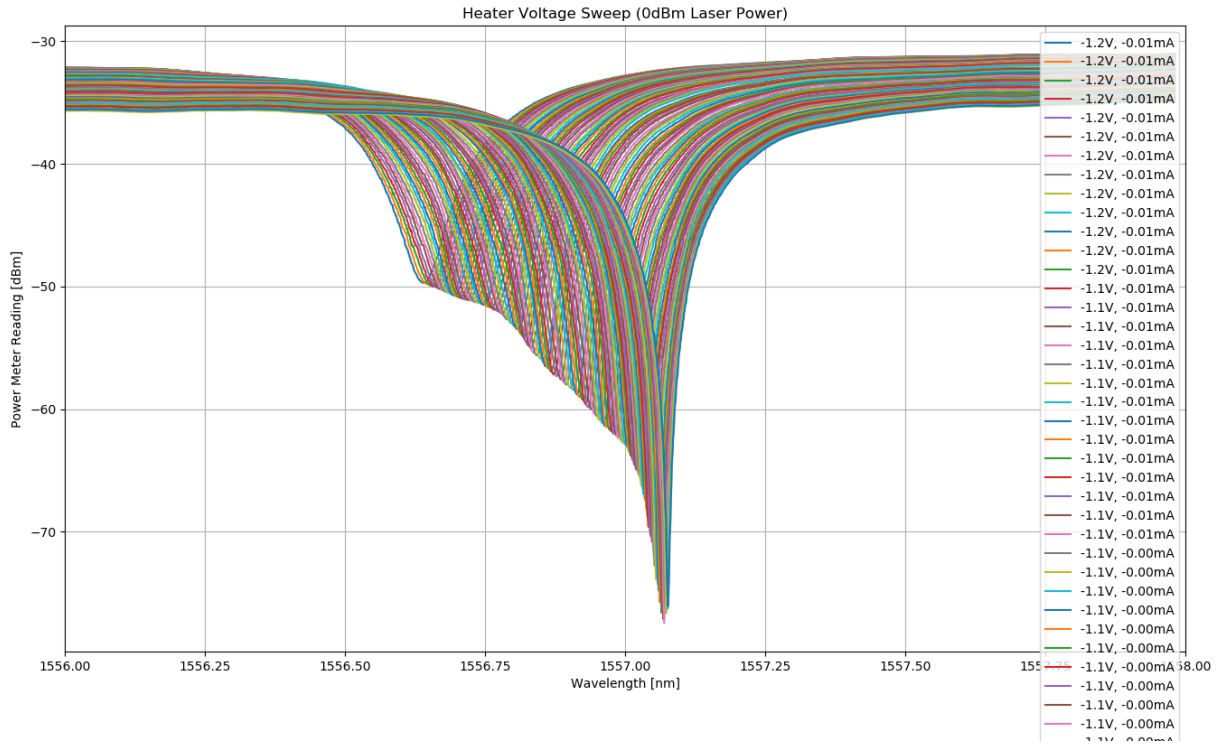
Figure 2: Example heater voltage sweep.

The plots below are the output power vs. the input laser wavelength sweeped at various bias voltages. What is important to notice is that the transfer characteristic resembles something similar to a Lorentzian function. This will be useful in modeling the ring in future sections to make distortion calculations simpler. Note that the legend in figure 2 is truncated so each data point is taken at a different input bias voltage.

2 High Level Simulations

2.1 Modeling the Ring as a Lorentzian

Figure 3: A generic Lorentzian function plot
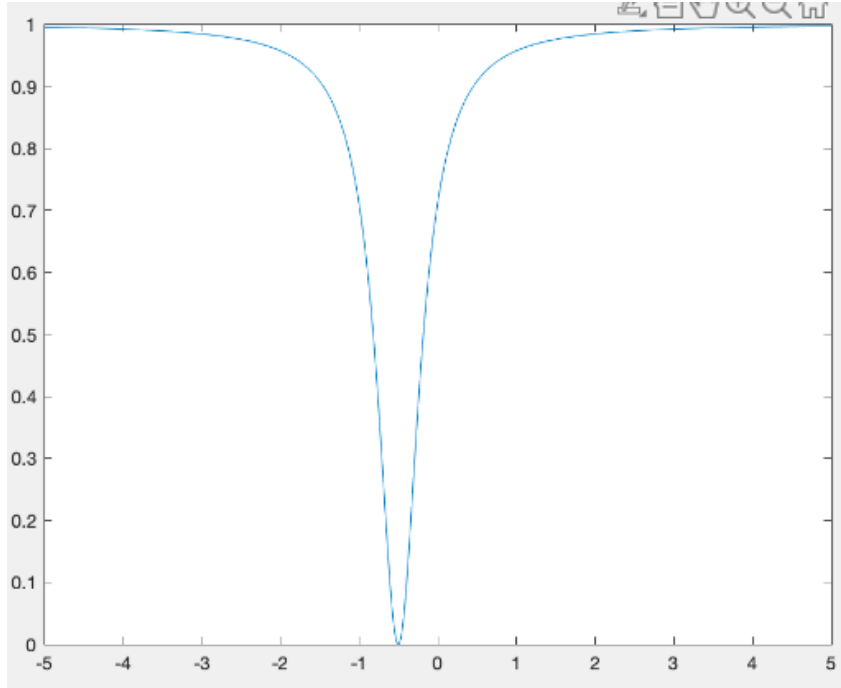
As seen above, the Lorentzian function is useful in modeling the overall transfer function of the RRM. The laser frequency versus output power of the ring roughly resembles the shape of the Lorentzian curve above. Applying a bias voltage to the ring shifts the entire curve to the left or right based on the polarity of the bias. Therefore, the basic idea is to ensure that the bias point of the ring(i.e the DC bias voltage applied to the ring) is at a point on the curve in which it looks roughly linear. For the sake of simulation, the Lorentzian used to model the ring is offset by -0.5V such that the small-signal AC signal is biased at a spot(x=0) that is roughly linear.

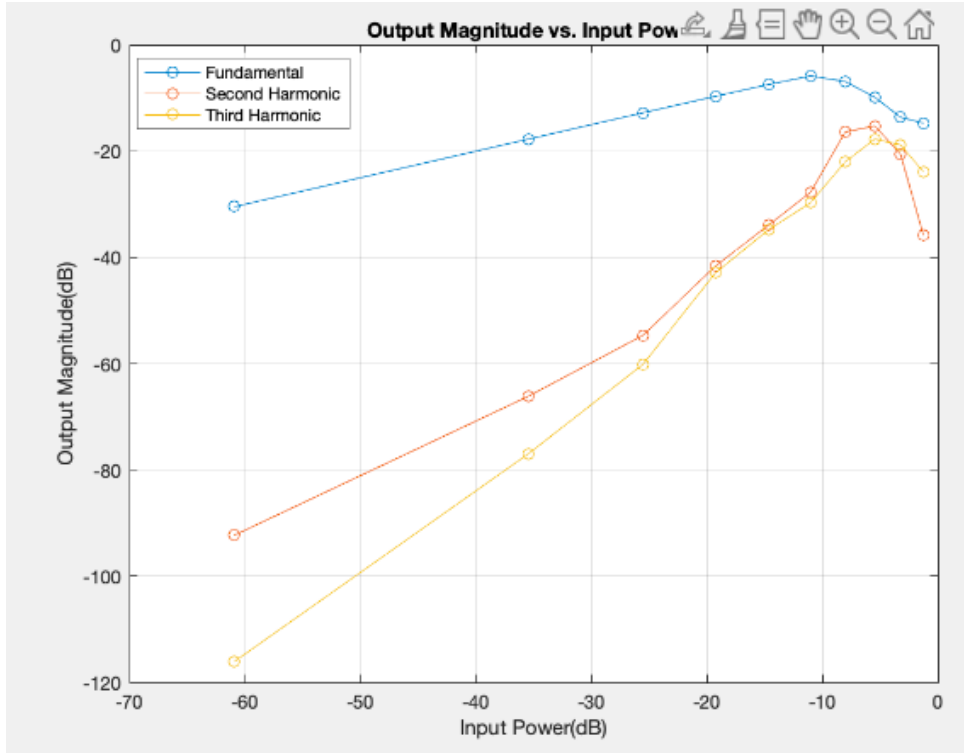## 2.2   Simulating Harmonic Distortion

Figure 4: Output Power vs. Input power for Various Harmonics of Lorentzian

The first simulations involved measuring the open-loop harmonic distortion of the non-linear Lorentzian function. More than anything this served to ensure that the Simulink environment was properly configured and that the results obtained matched the expected theoretical distortion values. Measuring the open-loop harmonic distortion would also be useful in examining the effects of adding a feedback loop and any potential benefits or drawbacks of doing so. As seen in later sections, the second and third harmonic distortion factors are reduced by adding feedback. In other words, by adding the feedback loop around the nonlinearity(in this case a Lorentzian function), the overall response of the ring will become more linear.

As seen above, the first, second and third harmonics of the Lorenztian curve follow the pattern one would expect. The linear slopes of each of the harmonics follows a ratio of 1:2:3 respectively due to the fact that this graph is a log-log plot.
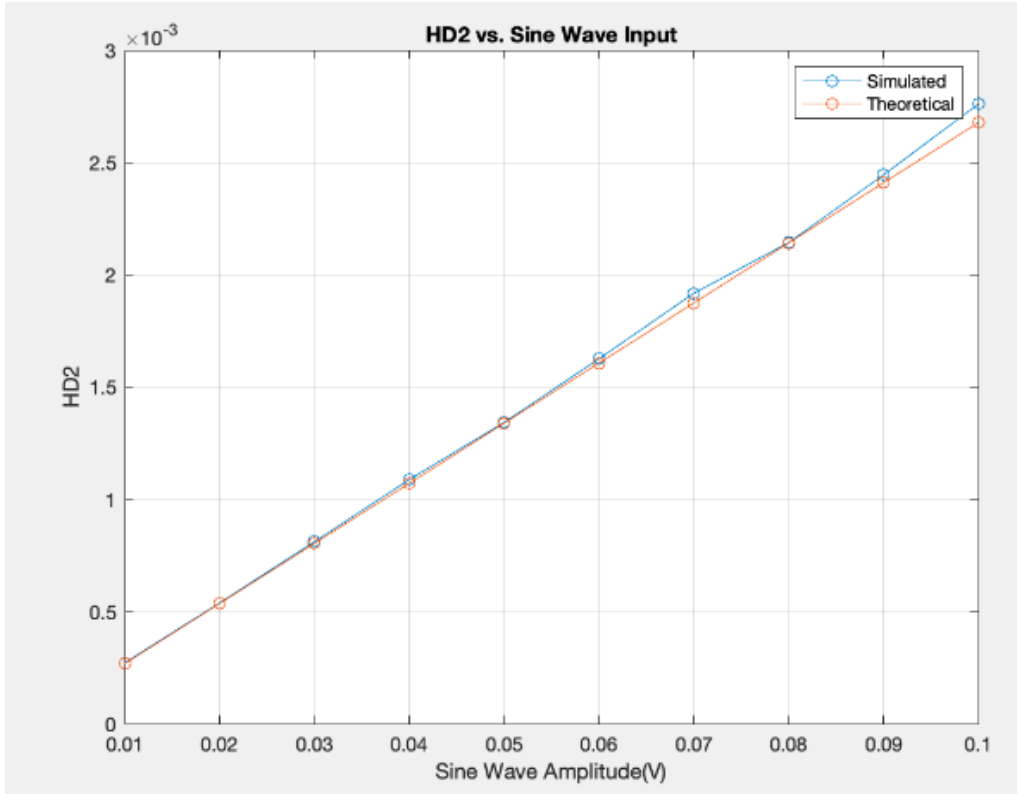
Figure 5: HD2 of Ring Modeled as a Lorentzian Function(In Open Loop)

As seen by figure 5, the HD2 of the ring almost exactly matches the theoretical values of HD2 calculated by hand. These hand calculations of HD2 used the equations enumerated below. To clarify, a_1, a_2, etc are the coefficients of the Taylor series expansion of the Lorentzian function and $s_o m$ is the magnitude of the output signal. T is the value of the DC loop gain. This is a good sign because it confirms that in Simulink we are modeling the ring as a pure Lorentzian function and nothing else.

1.

$$HD2_{open} = \frac{0.5 a_2 s_{om}}{a_1^2}$$

2.

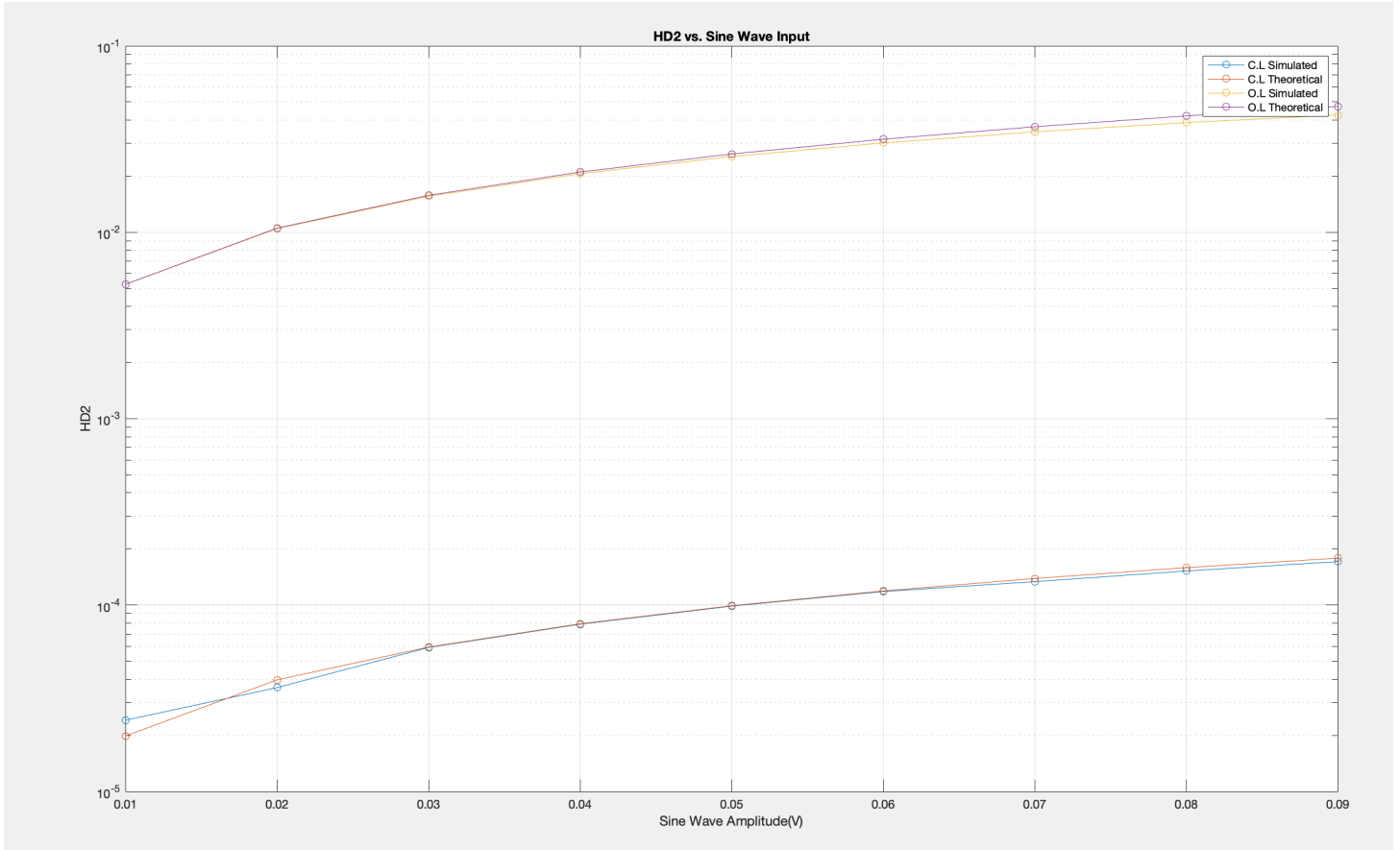$$HD2_{closed} = \frac{0.5 a_2 s_{om}}{a_1^2 (1 + T)}$$

Figure 6: Simulated and Hand Calculated HD2 for an Open and Closed Loop Setup

After the open loop measurements of HD2 were found, the closed loop values were found in a similar fashion. The experimental closed loop values of HD2 were found by first taking an Fourier transform of the outputted signals from the Simulink simulation and extracting the magnitudes of the fundamental and second harmonic. These were compared and plotted alongside the calculated closed loop HD2 values(see figure). As seen by the figure, feedback lowers second harmonic distortion by a factor of about the loop gain.

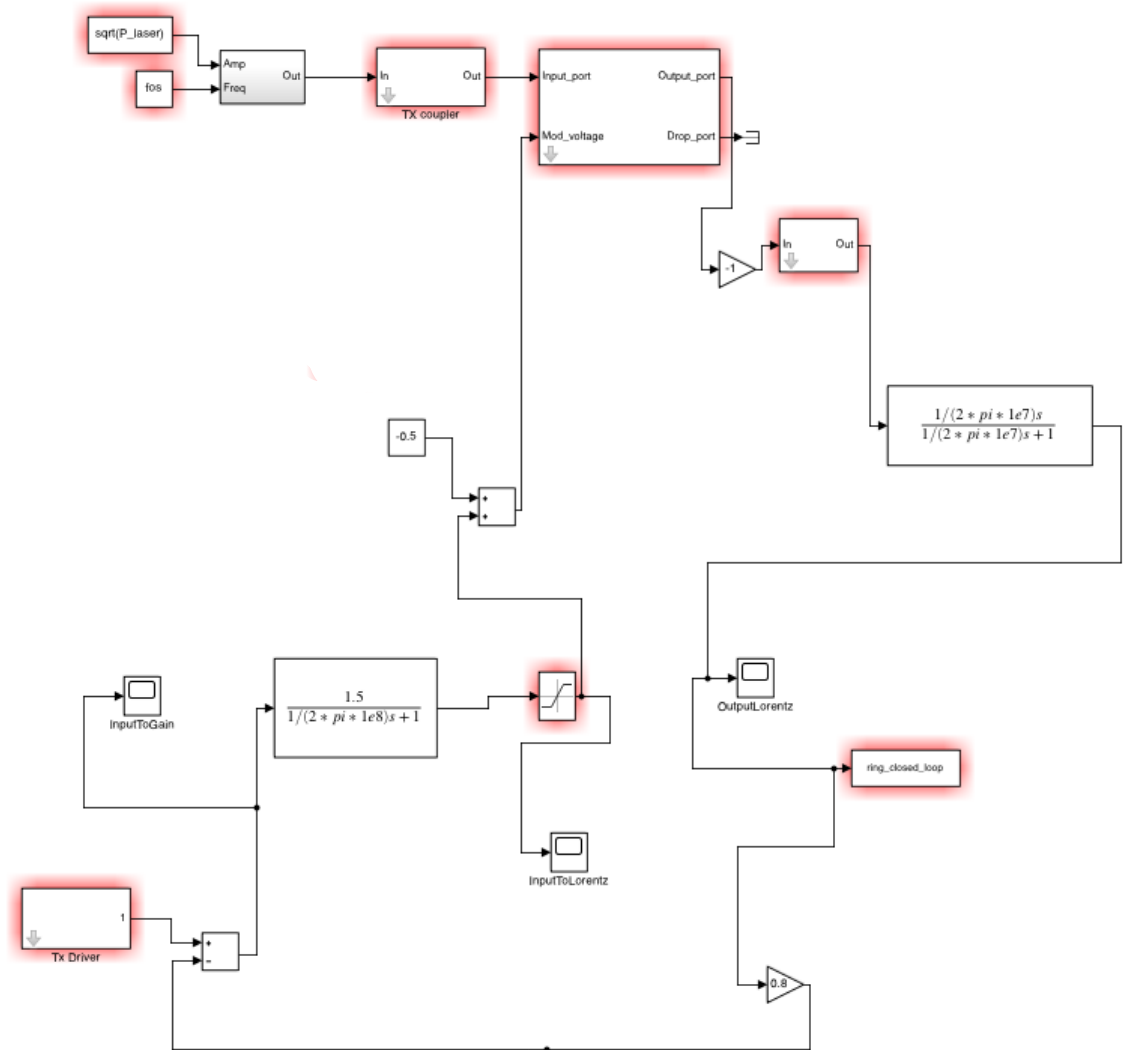## 2.3 Simulink Modeling with the Ring Model

Figure 7: The full Simulink Feedback loop

The next step in getting a complete picture of the feedback loop is to replace the Lorenztian function which stood as a model for the ring with an actual ring resonator model in Simulink. The feedback loop consists of a forward gain block, the ring model itself, and a feedback factor which loops the signal back into the add block on the bottom left. Note that a high pass filter was used at the output of the ring photodetector in order to remove any DC offsets produced from the ring model itself. At the input side of the ring model, a bias voltage(-0.5V for this particular model) was added to the signal path because the ring needs to be biased in the linear looking regions of its transfer function, and since we filter out DC biases at the output this DC value must be injected in before the signal path reaches the ring itself.

3 Circuit Level Simulations

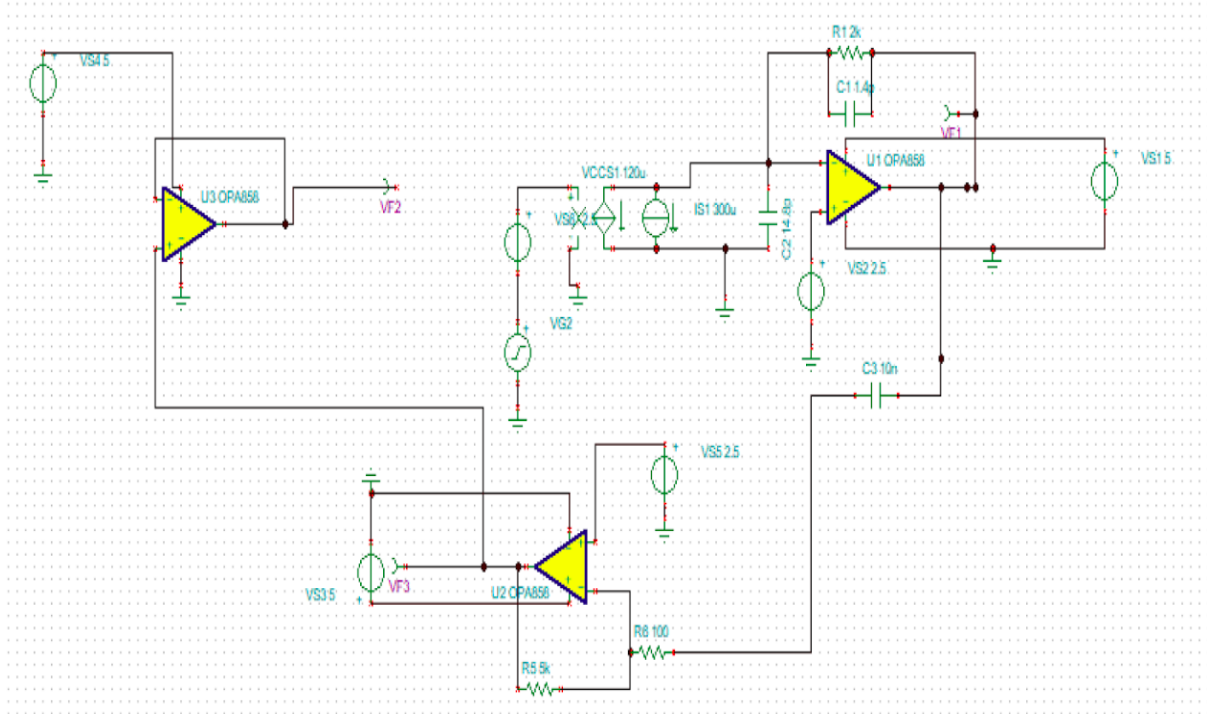## 3.1 Simulating the entire feedback loop in Tina-TI

Figure 8: The full TINA-TI Feedback loop

An OPA858 high speed op amp was used to construct the circuits needed for the TIA, voltage buffers and amplifiers present in the loop. In order to simulate this specific op amp, the TINA-TI circuit simulator was used to model the feedback loop. The ring itself can be seen as simply a Voltage Controlled Current Source(VCCS), where the input voltage produces some output current from the photodetector. Note that there is a current source at the output of the VCCS that represents the DC bias current that will flow out of the ring. Similarly, the input bias voltage(2.5V) is subtracted off before the VCCS in order to prevent double counting the bias point of the ring. The output current of the ring is then fed into the TIA which converts it into a voltage. The next stage is an inverting amplifier that serves as an error amplifier between the input modulation voltage and the feedback signal. The output of the error amplifier is then fed into a final buffer stage which is fed back into the ring. For stability analysis, the loop is broken at the high impedance input node of the VCCS as seen in the figure above.

It is important that the feedback loop is biased properly to ensure the maximum headroom possible. Thus, a 2.5V reference voltage is fed into the positive inputs of the TIA and inverting amplifier op amps. This sets the DC bias to 2.5V for all nodes in the circuit except the output of the TIA, which is biased at 3.3V. This is due to the DC bias current of 300uA that flows through the feedback resistor of the TIA.
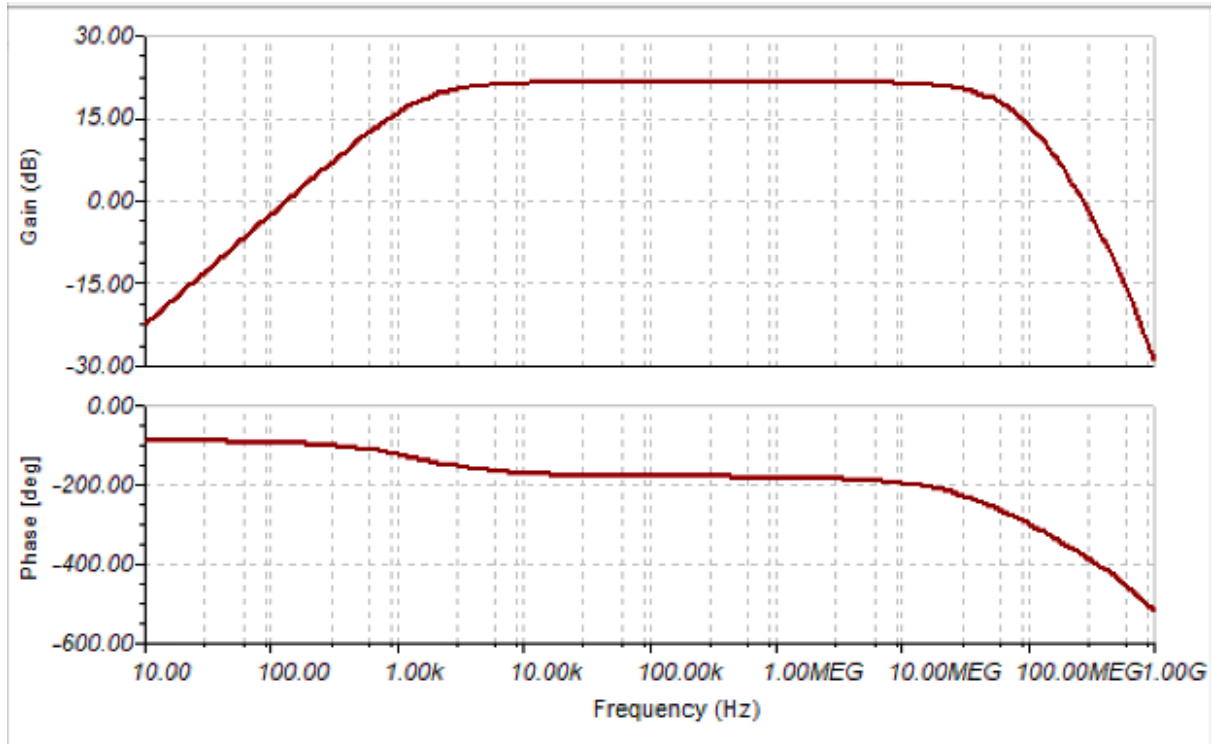
Figure 9: AC Analysis of the TINA-TI Model

Running an AC analysis yielded a bandpass with a total bandwidth of about 2 MHz. The midband frequencies range from 2 kHz to 20 MHz. The midband loop gain was designed to be about 10 V/V, or 20 dB, which is reflected in the AC results above. Note that the phase at midband is -180 degrees, which at first glance may indicate instability. However, this phase is expected due to the inverting amplifier stage, which essentially flips the feedback signal. Due to the location where the loop was broken for the AC analysis, the input signal will actually be reduced when added to the 180 degree shifted feedback signal, thus making the loop stable as desired.

4 Building the Physical Circuits

The next step after running high level Simulink simulations is to begin building out different circuits that will be necessary in constructing the feedback loop in hardware. The overall physical loop is broken into three different boards, namely a TIA board, an error amplifier or compensator board, and a driver board. The TIA board will take the currents that are outputted by the ring photodiode and convert it into a voltage signal biased at mid-rail(2.5V). The error amplifier board will contain a differential amplifier which will take our input modulation signal as well as the feedback signal from the TIA as inputs. The output of this error amplifier board will be fed into a driver board, which will act as a simple voltage buffer that will drive the modulation port of the ring.

The software used to design and layout the boards was EagleCad. Below is an example of a board file containing the layout for the TIA board.
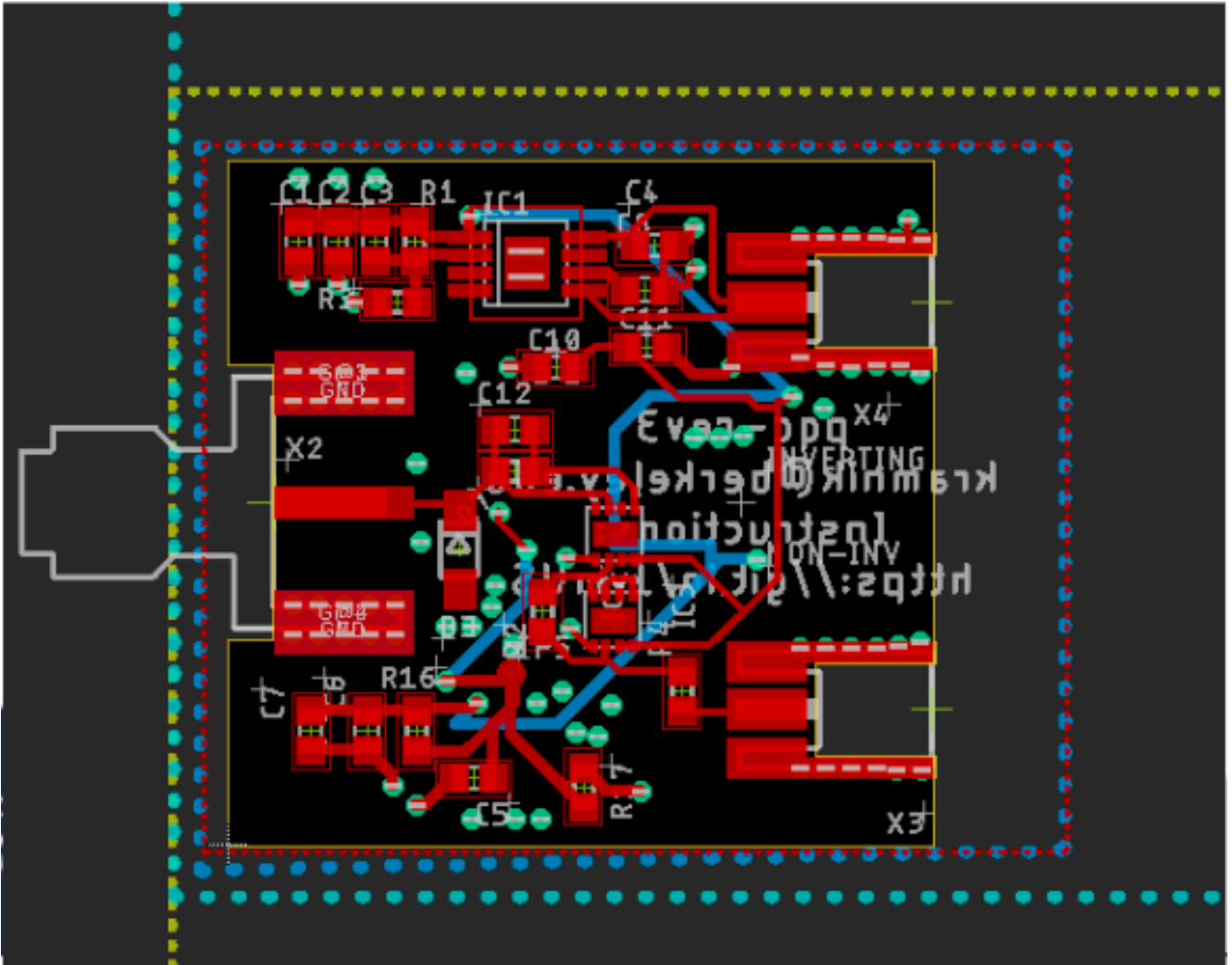
13

Figure 10: Eagle Cad Board file

4.1 Designing the TIA Board

The TIA board consists of an operational amplifier(opamp) and a feedback network consisting of simple resistors and capacitors. The main concerns when designing a TIA involve compensating it(making sure its poles and zeros are at desirable frequencies) and making sure its bias point is near mid-rail(2.5V). An example TIA schematic can be seen below. The values for the resistors and capacitors values in this schematic were used in the TIA design and changed in order to meet stability specifications. In order to find the transfer function of the loop gain of the TIA and measure its stability, it is necessary to know its forward gain and its feedback factor. The forward gain factor can be found by examining the open loop transfer function of the opamp, in our case an OP858 designed by Texas Instruments. The feedback factor is found by looking at the feedback network surrounding the opamp. In this case the feedback factor is simply an impedance divider between the output and negative input of the opamp.
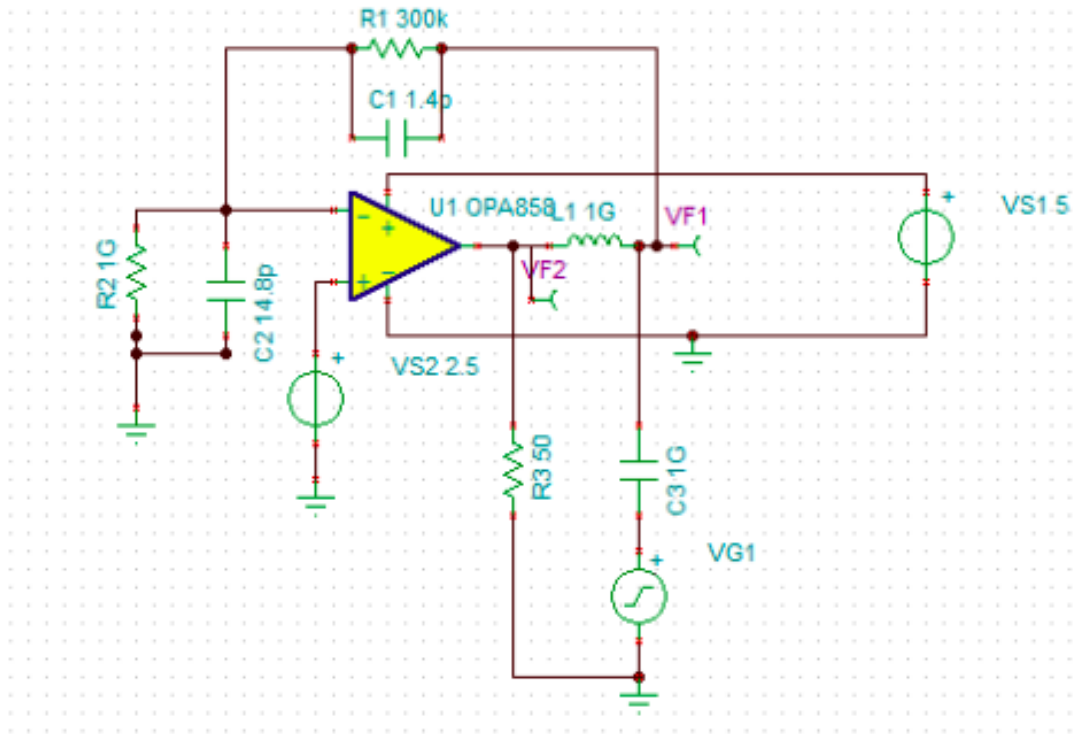
Figure 11: The finalized TIA design in TINA-TI

Note that for this project a high speed opamp must be used in contrast to a more standard opamp such as the 751. As seen in figure 11 above, the TIA designed for this project uses an OPA858. Like stated before, the first step in designing a stable TIA is to find the open loop transfer function of the opamp.
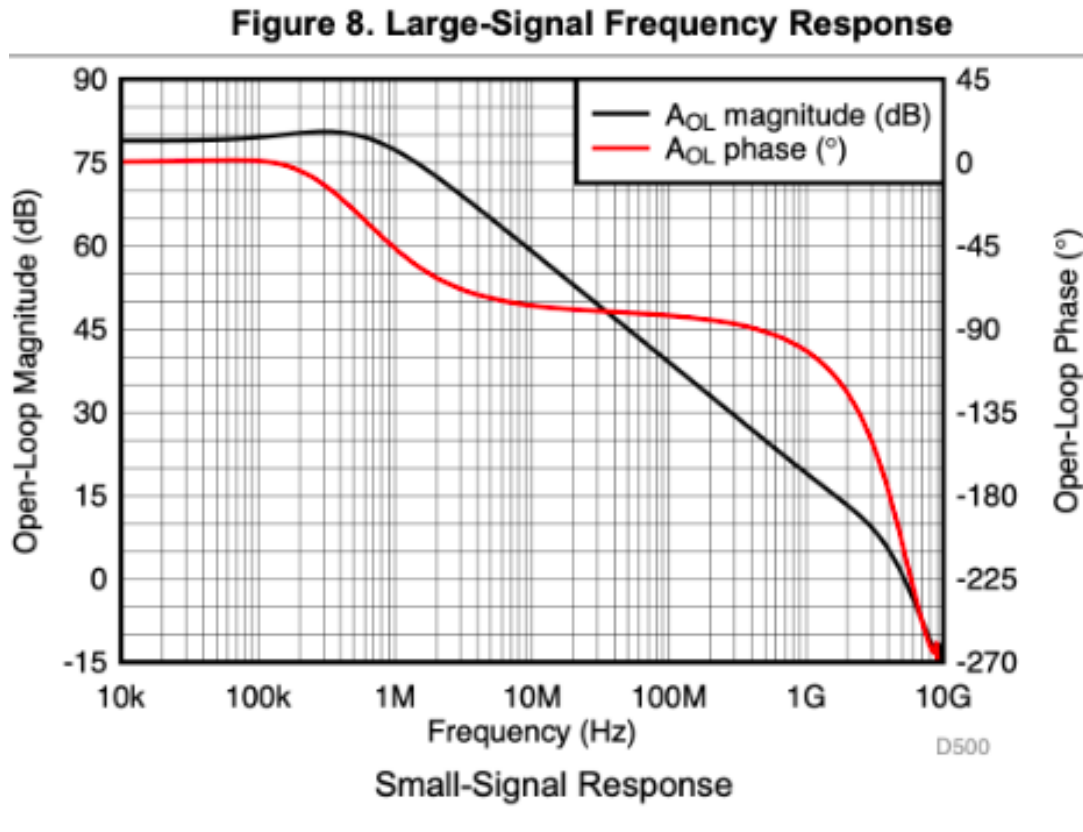
Figure 12: OP858 Open Loop Response

Figure 12 depicts the poles and zeros, as well as the phase of the OP858 at various frequencies. This is used to find its transfer function. This transfer function is then multiplied with the impedance divider from the output to negative input to find the loop gain of the TIA. The two transfer functions are as follows:

1.

$$A(s) = \frac{10000}{(1 + \omega/(1*10^6))(1 + \omega/(5*10^9))^2}$$

2.

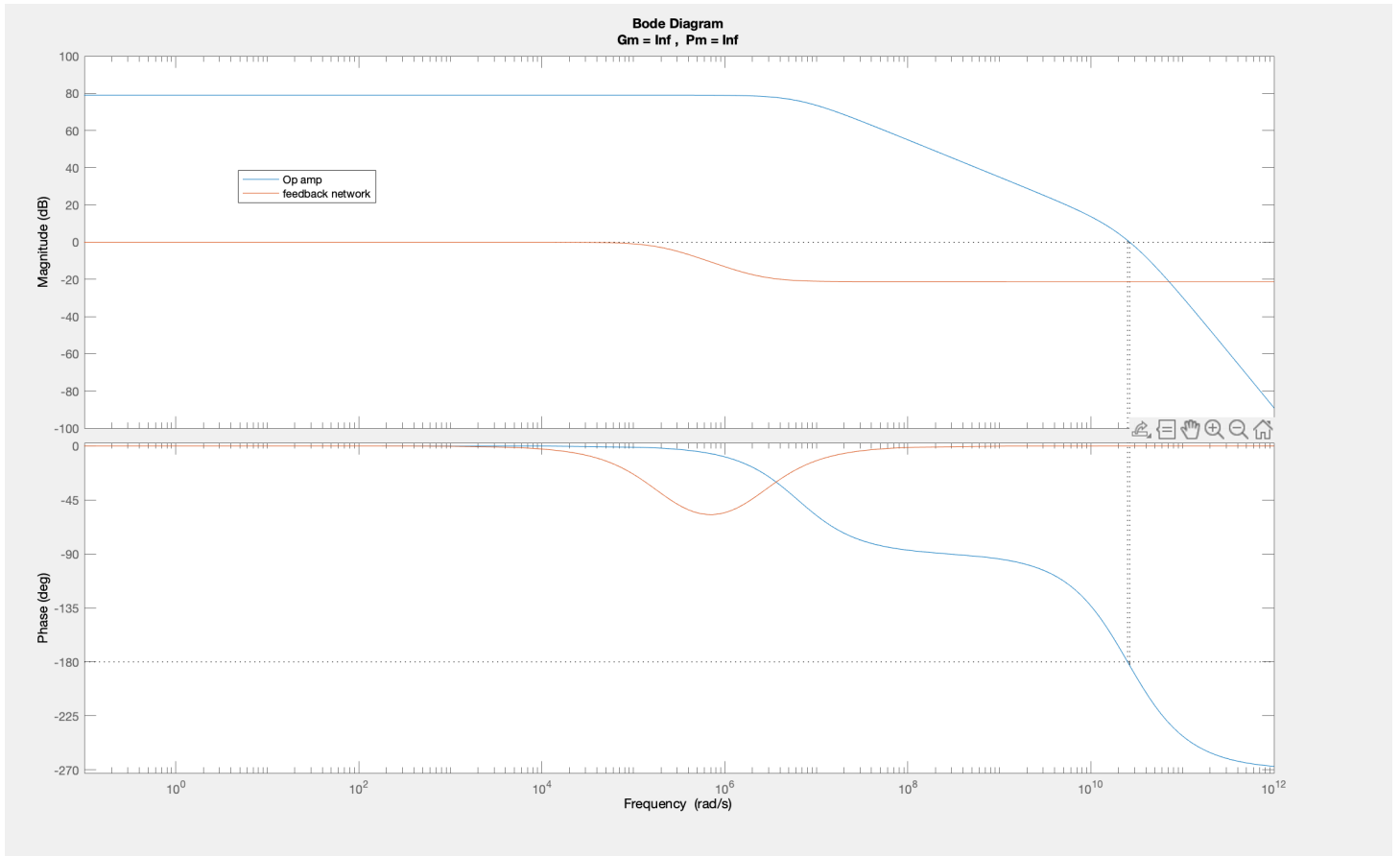$$f(s) = \frac{R_2||C_2}{R_2||C_2 + R_1||C_1}$$

16

Figure 13: OPA858 and Feedback Network Bode Plots in Matlab

Figure 13 depicts the open-loop opamp transfer function in blue and the feedback factor(impedance divider) transfer function in orange. Note that these plots are theoretical values from the equations that were enumerating above.
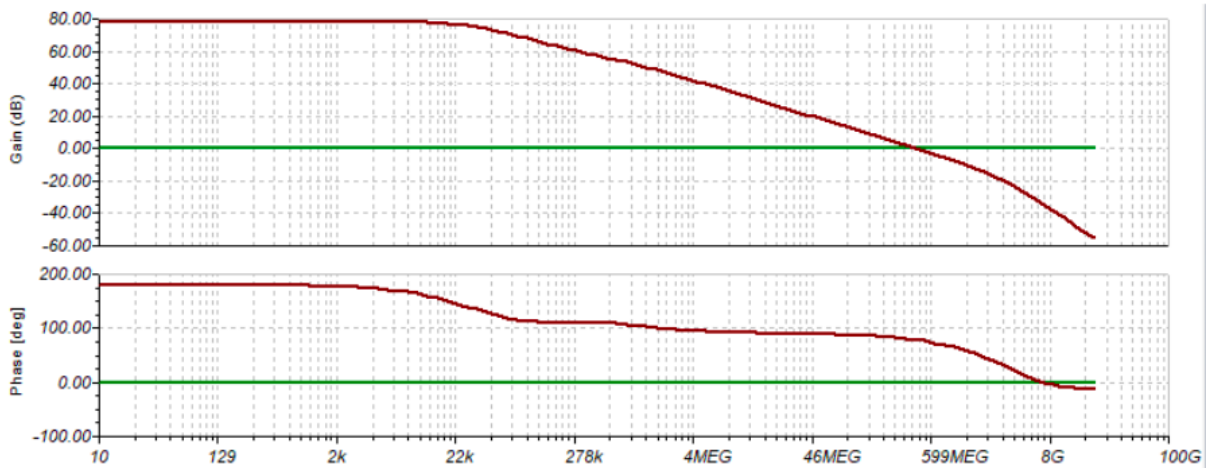
Figure 14: OP858 Open Loop Response and Feedback Factor Response(TINA-TI)

The resulting bode plots of the feedback network as well as the open-loop response of the opamp were plotted in matlab and observed(See figure 13). With the two transfer functions, it is possible to multiply them together and observe the loop gain bode plots. These hand calculation values were compared to and matched with TINA-TI simulation results. As seen in figure 14, the TINA-TI simulations show that the final design of the TIA has a DC loop gain value of 80dB with about 60 degrees of phase margin. Therefore, the TIA should be stable and functioning within the feedback loop.

4.2   The TIA Board

Figure 15: Physical TIA Board

As seen in figure 15, the TIA board consists of 3 inputs/outputs. There is one SMA input on the left hand side for the signal into the TIA which will come from the ring's photodiode. There is also an MMCX input(top right) for the power into the board. This

18

will be a 5V power supply that will power the regulators as well as the opamps on the board. Finally, there is an MMCX output(bottom right) which will serve as the output of the TIA.
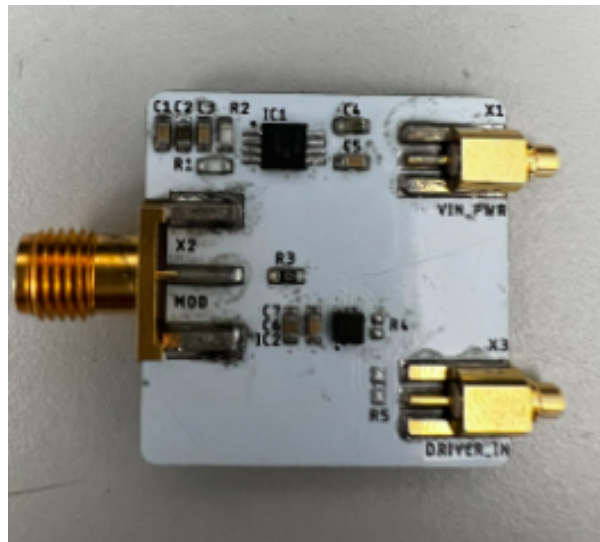
4.3 The Driver Board

Figure 16: Physical Driver Board

The driver board(figure 16) is very similar to the TIA described in the previous section. There is one SMA input on the left hand side and an MMCX power supply input on the top right. On the bottom right there is an MMCX output.
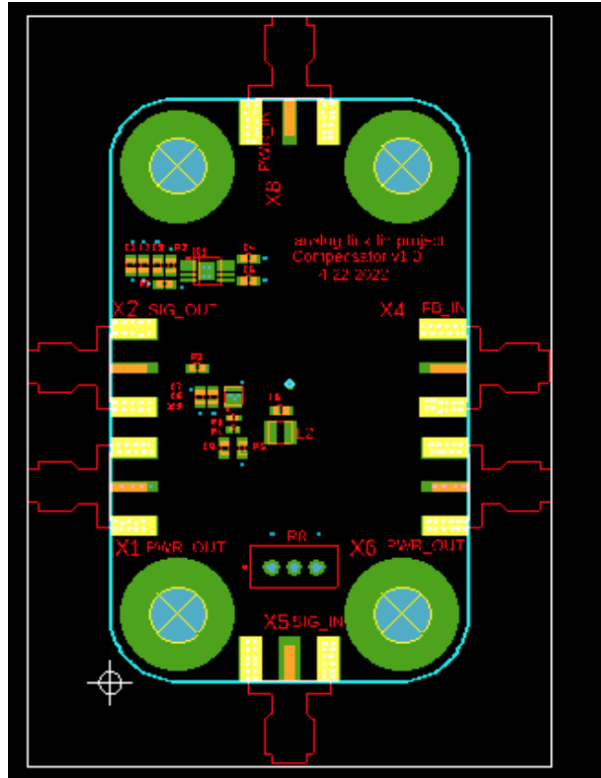
4.4 The Compensator Board

Figure 17: Compensator Board Layout

The compensator board is slightly different from the rest of the boards because it has two 5V supply outputs to power the other two boards as well as its own power input port. It also contains an input port for the modulation voltage input for the entire feedback loop. Finally, it contains an input port for the feedback signal from the TIA and an output port for the input of the driver board. The circuits on this board are quite simple, consisting of an OPA858 in an inverting amplifier configuration.
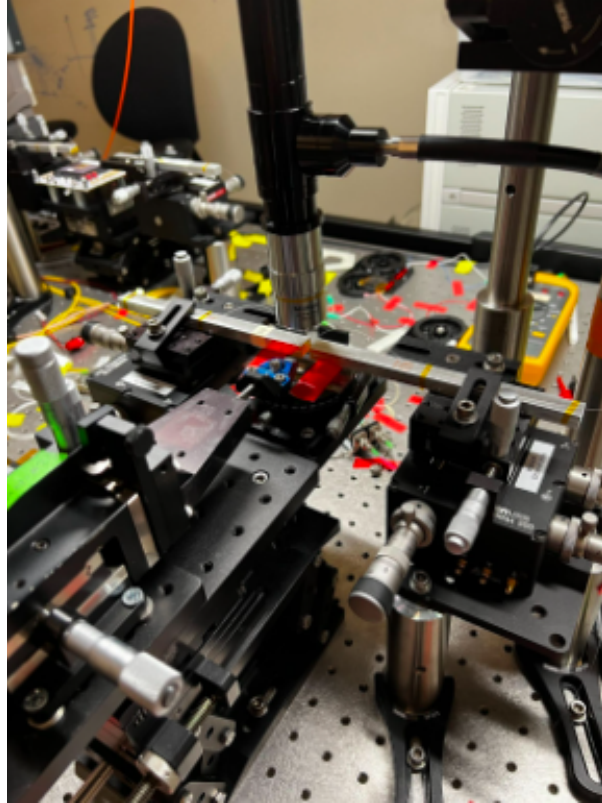
4.5 Testing the TIA

Figure 18: TIA testing setup

After performing surface mount soldering on the TIA board and before constructing the entire feedback loop, it is necessary to test the TIA board separately to ensure there are no shorts or other irregularities with it. Figure 18 depicts the test setup for the TIA board. The test chip which contains the ring itself is held in place with tape. The chip that was used for testing this board is the Shasta-T chip. Additionally, two fiber optic cables, one for carrying the laser input into the ring and one for detecting the output from the ring, are also aligned and landed onto the chip. The input fiber optic cable is connected to a Santec550 laser diode and the output fiber is connected to an Agilent Powermeter(not shown in the figure). The blue piece near the middle of the figure is a SG100 probe, which is landed on the photodiode of the ring in order to detect an output signal from the drop port. An important detail to note is the polarities of the probe as well as the photodiode on the chip. In order for the photodiode to function correctly, it must be configured in reverse bias. This implies an SG100 probe must be used. Note that a SG100 probe has probe tips spaced at 100um apart, which is the distance that the pads are spaced apart on this particular chip.
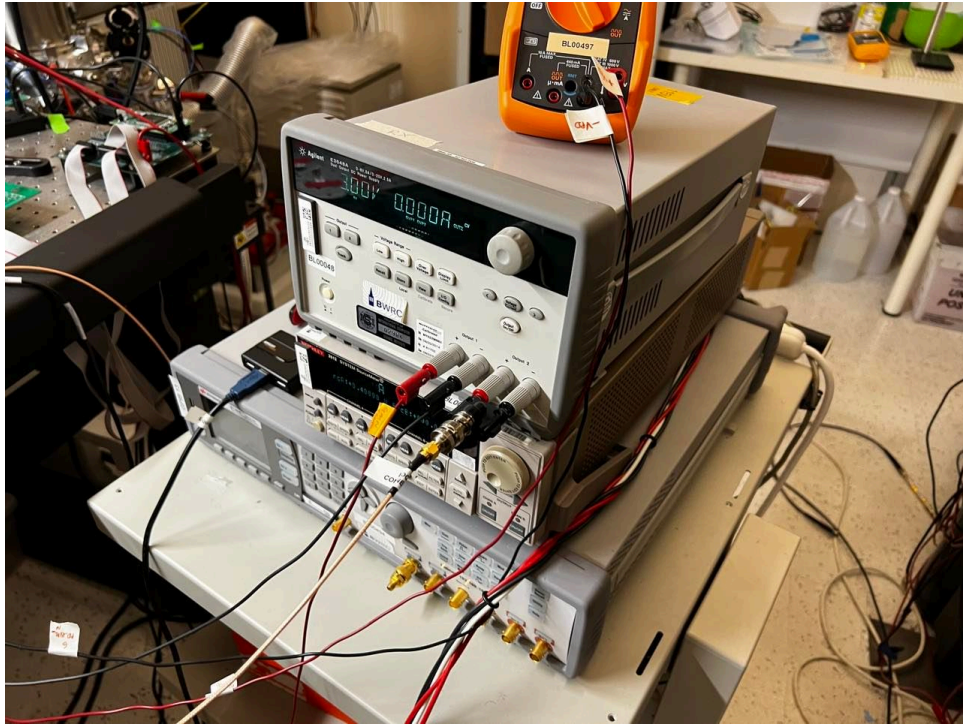
Figure 19: Sourcemeter, Power Supply, and Multimeter for TIA testing

In order to ensure that the probe has landed properly onto the chip and is functioning, a sourcemeter was used to apply a voltage to the probe. Since the probe is landed on a photodiode in a reverse bias configuration, the expected behavior should be to see large currents when a negative voltage is applied, and essentially no current when a positive voltage is applied. Once this was confirmed, a power supply was used to supply 5 Volts to the TIA board and the output was measured using a standard multimeter.

Before diving into the specifics of the results of measuring the TIA board, there are some extra caveats about the testing setup that must be taken into consideration. Note that an SG100 probe is required to measure the rings. This is due to the placement of the photodiode pads on the chip, where reverse bias corresponds to the signal being the left pad and the ground connection being the right pad. Many of the probes available were GSSG100 probes. It may seem logical to land the SG portion of the GSSG probe on the pads and leave the GS pins unconnected, however, a 4 pin probe is very hard to land on most chips due to an additional layer that coats the chip. The GS portion of the probe will hit the chip first and prevent the SG portion from landing. Therefore, if possible, avoid using a GSSG100 probe and find or purchase a SG100 probe.

Additionally, when searching for RF probes, it is necessary to be mindful of the connectors that the probe requires. Even if two probes are SG100, there is a chance that they require different connectors depending on their frequency specifications. For this application, a low frequency is sufficient.
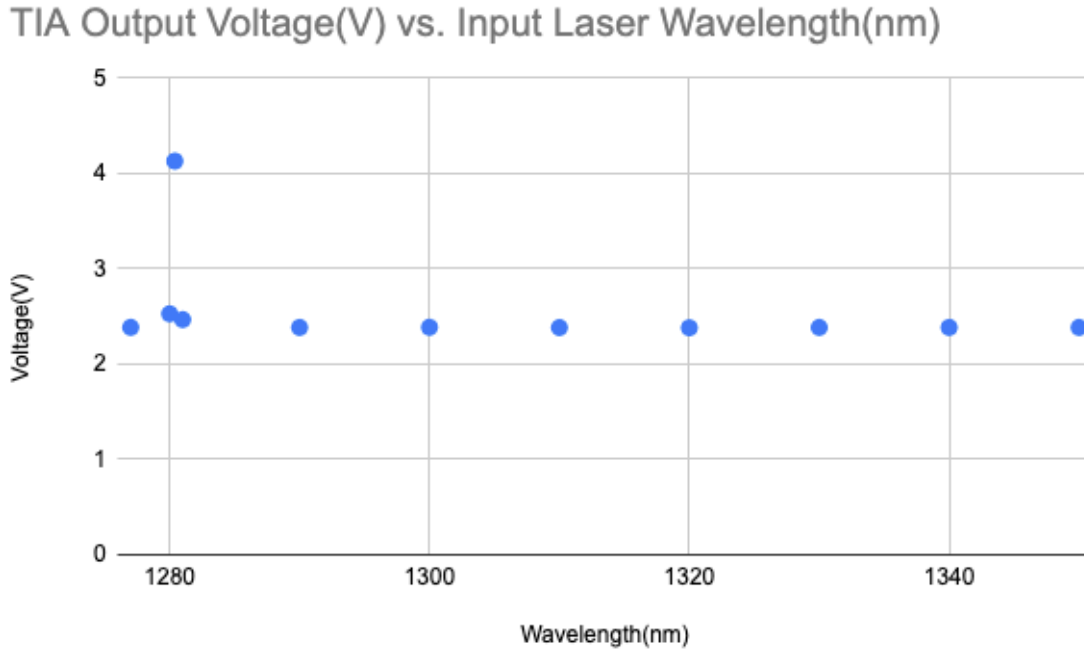
4.5.1 TIA Testing Results

Figure 20: TIA Voltage Output vs. Laser Frequency

As seen by the figure above, the TIA output voltage was measured as a function of the input laser wavelength. Note that the resonance frequency of the ring used lies around 1280.4 nm. At the resonance frequency, the output voltage spikes to around 4.13V since most of the power is being transmitted out of the drop port, which is what the ring PD is measuring.

5 Moving Forward

5.1 Next Steps

With the TIA completed and tested, the next step will be to construct the entire feedback loop and test it. Unfortunately, the test setup used for testing the TIA is not compatible with testing the entire feedback loop. The primary reason is the optic fiber setup is not conducive to landing two different probes. There simply is not enough room to land 2 probes alongside landing the fibers. With this in mind, a new test setup will need to be constructed. Another issue that will need addressing is the probes. Two SG100 probes will be needed and at the moment the lab only has one functioning probe, so more will need to be ordered. The final major change will be to order the correct female MMCX connectors for the driver and TIA boards since BWRC only has female MMCX to SMA cables. Male MMCX connectors were accidentally ordered and soldered onto the boards so those will need to be removed and replaced with the correct connectors. Alternatively, alternate male MMCX to SMA cables must be ordered.

5.2 Conclusion

There were many challenges associated with building a ring resonator feedback loop but ultimately the boards and design work needed were completed in the span of a year. The

results from simulation are promising in making the linearity of the ring resonator much better for MRI applications in the future.

References

[1] Bogaerts et. al (2011) *Silicon Microring Resonators*, Laser Photonics Reviews.

[2] Hosseinzadeh, Arash, "LINEAR RING RESONATOR MODULATOR FOR MICROWAVE PHOTONIC LINKS", Open Access Dissertation, Michigan Technological University, 2018.